

# A joint background field removal and dipole deconvolution approach for quantitative susceptibility mapping in the liver

Samir D. Sharma<sup>1</sup>, Diego Hernando<sup>1</sup>, Debra E. Horng<sup>1</sup>, and Scott B. Reeder<sup>1,2</sup>

<sup>1</sup>Radiology, University of Wisconsin - Madison, Madison, WI, United States, <sup>2</sup>Medical Physics, University of Wisconsin - Madison, Madison, Wisconsin, United States

**Target Audience:** Researchers who are interested in quantitative susceptibility mapping.

**Purpose:** Noninvasive quantification of liver iron concentration (LIC) is important for the detection, staging, and treatment monitoring of iron overload. Current relaxometry-based methods (i.e. R2 and R2\*) have good correlation with LIC<sup>1-3</sup>, although their relationship with LIC is empirically derived<sup>4</sup>. Magnetic susceptibility is a fundamental property of tissue that has a well-defined relationship with iron concentration<sup>5</sup>. Quantitative susceptibility mapping (QSM) methods have been developed in the brain to quantify the concentrations of localized iron deposits<sup>6,7</sup>. However, these methods have not yet been successfully applied to the liver, in part due to the presence of fat and motion in the abdomen, as well as rapid transverse signal decay in cases of severe iron overload (i.e. high R2\*). The purpose of this work was to develop and demonstrate the feasibility of a QSM technique for measuring susceptibility in the liver, which may serve as an imaging biomarker of liver iron overload.

**Theory:** QSM consists of estimating a local magnetic susceptibility distribution ( $\chi_L$ ) from a measured B0 field map ( $\psi$ ). The B0 field can be written as:  $\psi = \psi_L + \psi_B$  [1], where  $\psi_L$  is the local field, which is of interest, and  $\psi_B$  is the background field, which is composed of fields from the shim gradients and susceptibility sources outside of the imaging field-of-view. The local field can be expressed as:  $\psi_L = D\chi_L$  [2], where  $D$  represents the dipole response kernel. Current QSM methods formulate the estimation of  $\chi_L$  from  $\psi$  in two sequential and separate steps: 1) background field removal to isolate  $\psi_L$ , and 2) deconvolution of the dipole response kernel to estimate  $\chi_L$  from  $\psi_L$ . Recently, SHARP<sup>6</sup> has been proposed as an efficient method for background field removal. SHARP recovers the local field by solving the following expression:  $ML\psi = ML\psi_L$  [3] where  $L$  is a discrete Laplacian operator and  $M$  is a binary mask that defines the spatial region of reliable estimates after applying  $L$ . Because the operator  $ML$  is singular, regularization must be incorporated to estimate  $\psi_L$  in Eq. 3. The subsequent dipole deconvolution step estimates the local susceptibility distribution ( $\chi_L$ ) by solving Eq. 2. Because  $D$  is singular, regularization must be also incorporated into the estimation of Eq. 2. In this work, rather than estimating  $\chi_L$  via a sequential two-step reconstruction that may require two separate forms of regularization, we formulate a joint estimation by combining Eqs. 2 and 3, whereby  $\chi_L$  is related directly to the measured B0 field map ( $\psi$ ):  $ML\psi = MLD\chi_L$  [4]. To regularize the deconvolution, an edge-weighted ( $E$ ), 3D finite-difference ( $G$ ) penalty term is used<sup>7</sup>. This leads to the following reconstruction expression:  $\min_{\chi_L} \|ML(\psi - D\chi_L)\|_2^2 + \lambda \|EG\chi_L\|_2$  [5]. In this formulation, the background field removal and dipole deconvolution are performed jointly rather than in two separate steps.

**Methods:** In vivo studies were conducted after obtaining IRB approval and informed consent using a 1.5T scanner (GE Healthcare, Waukesha, WI). Multi-echo chemical shift encoded data were acquired from eight healthy subjects using a six-echo SPGR sequence and an eight-channel torso phased array. Full 3D coverage of the liver was realized in one breath-hold with the following scan parameters: TE<sub>1</sub> = 1.2ms,  $\Delta$ TE = 2.0ms, matrix size = 256x160x32, true spatial resolution of 1.4x1.6x8mm<sup>3</sup>, parallel imaging acceleration = 2x2. The B0 field map (as well as the water ( $\rho_w$ ) and fat ( $\rho_f$ ) images, and R2\* map) was estimated from the SPGR acquisition using a chemical species separation reconstruction<sup>8</sup>. The B0 field map is naturally corrected for the presence of fat when performing this reconstruction. The local susceptibility distribution,  $\chi_L$ , was estimated by minimizing the expression in Eq. 5 using linear conjugate gradients. A 3x3x3 Laplacian kernel was used to minimize the loss of field map information at the edge of the imaging volume. The edge-weighting mask,  $E$ , was generated using the image  $(\rho_w - \rho_f)/(\rho_w + \rho_f)$ , which clearly depicted edges in the anatomy while also being insensitive to variations in B1 coil sensitivity. The edge-weighting map was generated by assuming that 20% of the tissue pixels in the image were edges. The regularization parameter was chosen as  $\lambda = 3 \times 10^{-3}$  using two separate datasets. The susceptibility in the liver was measured with reference to the nearby subcutaneous fat, with a presumed susceptibility value of -7.79ppm<sup>9</sup>.

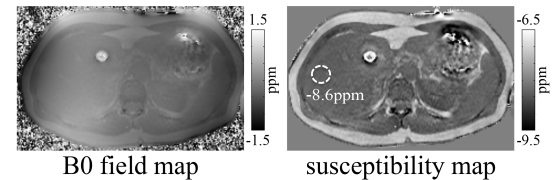


**Figure 1:** B0 field map and estimated susceptibility map for one of the subjects. The liver susceptibility measurement is taken with reference to the nearby subcutaneous fat.

**Results:** Figure 1 shows the B0 field map and the estimated susceptibility map from one subject. The liver ROI measurement is shown with respect to the subcutaneous fat. Figure 2 plots the estimated liver susceptibility value for the seven subjects. The results from one subject were excluded because the B0 field map was incorrectly estimated due to a water-fat swap. The liver susceptibility values are in close agreement with one another, and the difference between the subcutaneous fat and liver susceptibility estimates are consistent with values published in the literature<sup>5,9</sup>.

**Discussion and Conclusion:** We have developed a QSM reconstruction technique that jointly performs background field removal and dipole kernel deconvolution to estimate the local susceptibility distribution directly from the B0 field map. We have demonstrated the feasibility of this approach for measuring susceptibility in the normal liver, which may serve as an imaging biomarker of liver iron overload. Further work will test and validate this QSM reconstruction in patients with liver iron overload. The rapid transverse signal decay in cases of iron overload, which results from high R2\* in the liver, may require further refinement of the proposed approach.

**References:** <sup>1</sup>St. Pierre et al., Blood 2005;105:855-861. <sup>2</sup>Wood et al., Blood 2005;106:1460-1465. <sup>3</sup>Hankins et al., Blood 2009;113:4853-4855. <sup>4</sup>Hugre et al., MRM 2011;65:837-847. <sup>5</sup>Schenck, Med Phys 1996;23:815-850. <sup>6</sup>Schweser et al., Neuroimage 2011;54:2789-2807. <sup>7</sup>Liu et al., MRM 2011;66:777-783. <sup>8</sup>Reeder et al., MRM 2005;54:636-644. <sup>9</sup>Hopkins et al., MRM 1997;37:494-500.

**Acknowledgements:** We acknowledge support of the NIH (R01 DK083380, R01 DK088925) and the WARF Accelerator Program. We also thank GE Healthcare for their support.

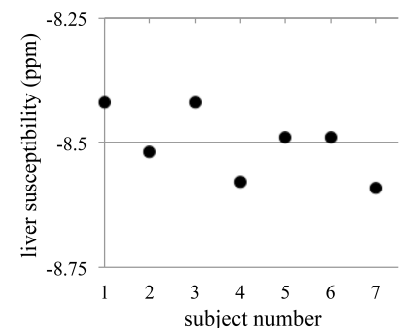


**Figure 2:** The liver susceptibility estimate for each of the seven subjects, with reference to the adjacent subcutaneous fat. The susceptibility values demonstrate good agreement with each other, and the values, relative to fat, are consistent with those published in the literature<sup>5,9</sup>.